

# Three-dimensional microfluidic devices fabricated in layered paper and tape

Andres W. Martinez, Scott T. Phillips, and George M. Whitesides

This article describes a method for fabricating 3D microfluidic devices by stacking layers of patterned paper and double-sided adhesive tape. Paper-based 3D microfluidic devices have capabilities in microfluidics that are difficult to achieve using conventional open-channel microsystems made from glass or polymers. In particular, 3D paper-based devices wick fluids and distribute microliter volumes of samples from single inlet points into arrays of detection zones (with numbers up to thousands). This capability makes it possible to carry out a range of new analytical protocols simply and inexpensively (all on a piece of paper) without external pumps. We demonstrate a prototype 3D device that tests 4 different samples for up to 4 different analytes and displays the results of the assays in a side-by-side configuration for easy comparison. Three-dimensional paper-based microfluidic devices are especially appropriate for use in distributed healthcare in the developing world and in environmental monitoring and water analysis.

**D**iagnostic devices for the developing world must be inexpensive, rugged, lightweight, and independent of supporting infrastructure (1–7). Among the most successful of current systems are those that rely on lateral movement of fluids across paper strips to distribute reagents (e.g., dipsticks and lateral flow systems) (2, 6). These systems are useful, but limited in their capabilities (2, 7). This article describes a new class of analytical devices fabricated by layering paper patterned into hydrophilic channels and hydrophobic walls (1, 8, 9) and tape patterned with holes that connect channels in different layers of paper. These devices extend paper-based assays from simple 1D lateral-flow systems to 3D devices with complex microfluidic paths, and expand significantly the capabilities of very low-cost analytical systems. There are many examples of 3D polymeric or glass microfluidic systems (10–14), but 3D paper-based systems combine simplicity in fabrication, complexity in fluidic and bioanalytical capability, and low cost. We believe they will be useful in a variety of applications, including diagnostics for developing economies, drug development, and environmental monitoring.

We call these devices 3D microfluidic paper analytical devices ( $\mu$ PADs). They distribute fluids both vertically and laterally, and they enable streams of fluid to cross one another without mixing. These devices use capillary wicking to distribute fluids into complex arrays of tens to thousands of detection zones in times of seconds to minutes (depending on the architecture of the device, and the choice of materials). The devices are small ( $<10\text{-cm}^2$  footprint), lightweight ( $0.15\text{ g}\cdot\text{cm}^{-2}$ ), and are easy to stack, store, and transport; they do not require external pumps, and they are thus appropriate for applications in: (i) innovative developing countries (IDCs) (15), as diagnostic and analytical devices that could be combined with telemedicine (1); (ii) array-based analytical systems in the pharmaceutical industry (but with lower cost and greater flexibility than currently used systems); and (iii) other analytical problems that require low cost, simplicity and ruggedness (e.g., in the military, homeland security, and monitoring the health of plants and animals).

## Results and Discussion

We fabricated 3D  $\mu$ PADs by stacking alternating layers of paper and water-impermeable double-sided adhesive tape (both patterned in ways that channel the flow of fluid within and between layers of paper) (Fig. 1A). The hydrophobic polymer patterned into the paper demarcated the channels through which the fluids moved laterally (8, 9), the layers of water-impermeable double-sided tape separated channels in neighboring layers of paper, and holes cut into the tape allowed fluids to flow vertically.

The layers of paper were patterned with SU-8 2010 photoresist. Paper was impregnated with photoresist, dried, exposed to UV light through a transparency mask, and developed with acetone and isopropyl alcohol (8, 9). The layers of tape were patterned using a laser cutter. The tape could also be patterned manually, using a hole punch, albeit much more slowly.

Once the individual layers of paper and tape were fabricated, we assembled them by stacking. A single layer of tape (with a protective film on one surface) was attached to a layer of patterned paper. The holes ( $60\text{-}\mu\text{m}$  thick  $\times \geq 800\text{-}\mu\text{m}$  diameter) in the tape were filled with a paste made from cellulose powder and water. The protective film was removed from the tape, and a second layer of paper was aligned and attached to its second surface. This process of stacking—paper, tape, paper, tape—was repeated as needed to complete a device, and provided a reproducible method for fabricating devices.\* The cellulose powder was used to fill the gaps between adjacent layers of paper that were created by the thickness of the tape. Without the cellulose powder, fluids did not wick reproducibly between two adjacent layers of paper.

The cost of the materials used to make the device shown in Fig. 1 was approximately \$0.03 or approximately \$0.003 per square centimeter per layer of paper and tape. For diagnostic applications, we use detection zones with 0.5–2.0 mm dimensions, so that the results of assays are easily visible by eye, and can be photographed accurately for cell-phone-based telemedicine (1).

Fig. 1 demonstrates the capability of 3D  $\mu$ PADs to move fluids in 3D; this demonstration system has 4 channels that cross one another multiple times in a basket-weave pattern. Aqueous solutions of dyes ( $20\text{-}\mu\text{L}$  aliquots) wicked the length of these channels in  $\approx 5$  min. Each continuous channel in this device was  $800\text{ }\mu\text{m}$  wide and  $\approx 5$  cm long, and included 8 connections between the top and bottom layers of paper.

Three-dimensional  $\mu$ PADs distribute samples from a single sample inlet on the top layer of the device into an array of spots

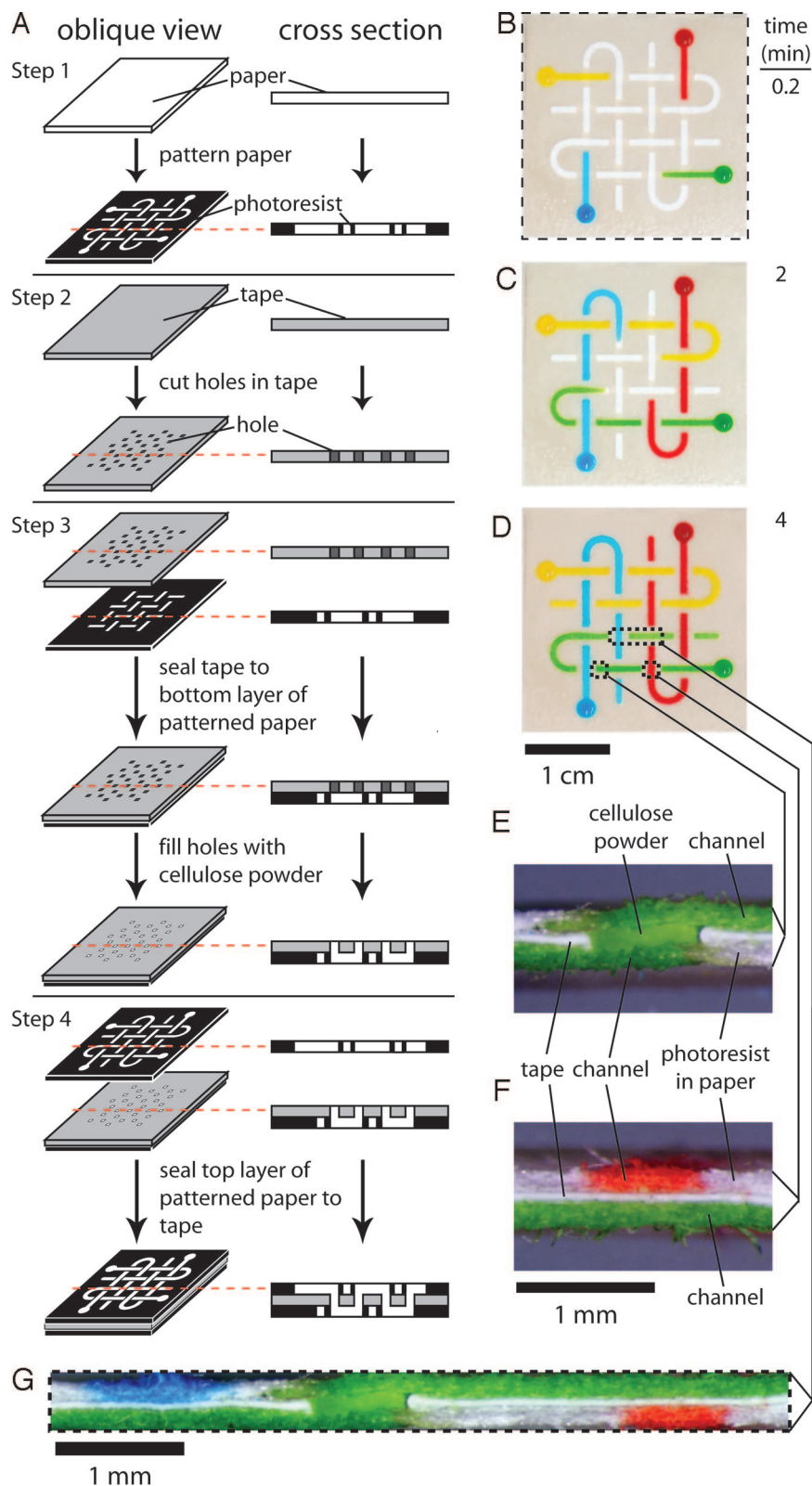


**Fig. 1.** Preparation and demonstration of a 3D  $\mu$ PAD. (A) Fabrication. (B) Photograph of a basket-weave system 10 s after adding red, yellow, green, and blue aqueous solutions of dyes to the sample reservoirs. The dotted lines indicate the edge of the device. (C and D) Photographs taken 2 (C) and 4 (D) min after adding the dyes. The streams of fluids crossed each other multiple times in different planes without mixing. The dotted lines in D show the positions of the cross sections shown in E, F, and G. (E) Cross section of the device showing a channel connecting the top and bottom layers of paper. (F) Cross section of the device showing the three layers of the device with orthogonal channels in the top and bottom layers of paper. (G) Cross section of the device showing the layers and the distribution of fluid (and colors) in each layer of the device shown in D. The dotted lines indicate the edges of the cross section.

or detection zones on the bottom layer of the device (Fig. 2). Reagents in these spots can detect multiple analytes simultaneously. The intervening layers of paper dictate the patterns of distribution from an inlet to a detection zone, and straightforward design provides easy access to different patterns.

Fig. 2 shows examples of devices with 4 sample inlets, and 64 detection zones. In these devices, the length of each fluidic channel connecting sample inlet and detection zones was equal ( $\approx 2$  cm) and ensured the distribution of equal quantities of sample into each zone. Fig. 2E is a device that distributed 4

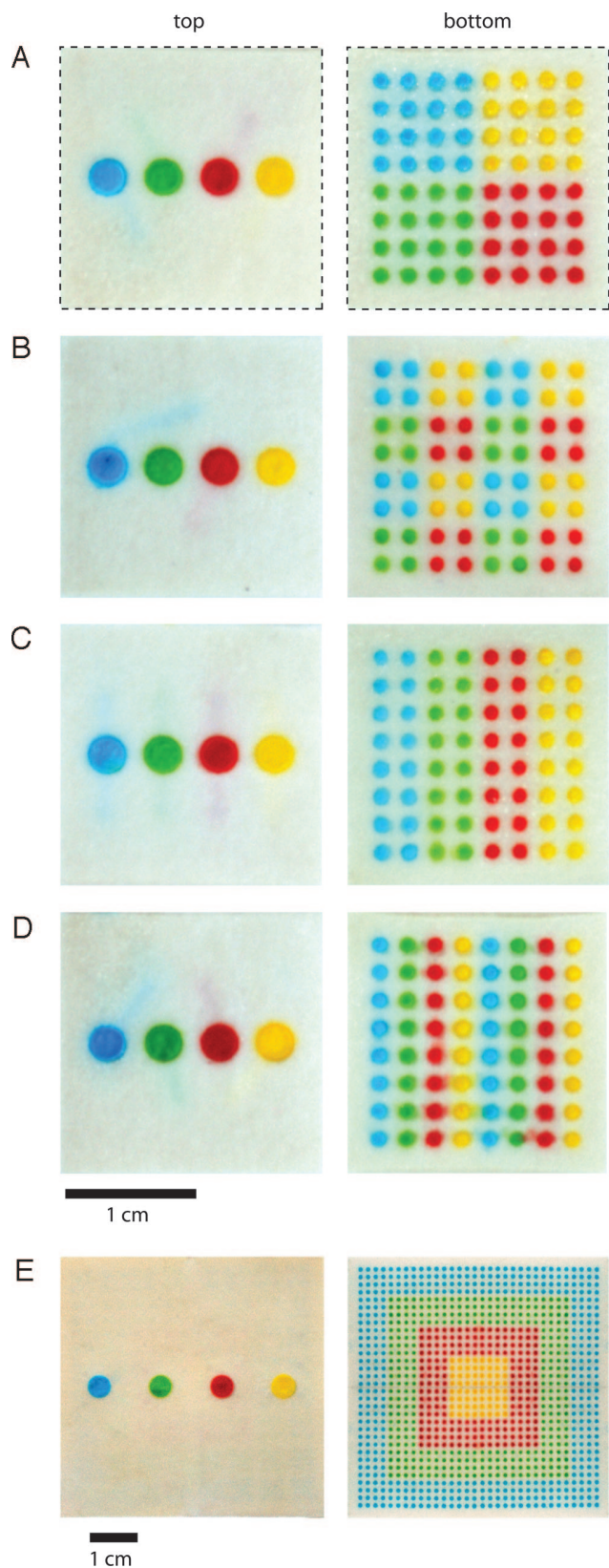


**Fig. 2.** MicroPADs that distribute fluids into arrays of detection zones. (A–D) Top and bottom photographs of devices that distributed each of four  $\approx 10\text{-}\mu\text{L}$  samples of fluids into 64 detection zones ( $\approx 4$  min). The dotted lines designate the edges of the devices. (E) Device that distributed  $\approx 100\text{-}\mu\text{L}$  of each fluid into 1,024 detection zones. Schematics of the layers making up the devices are shown in Fig. S1.

samples into an array of 1,024 detection zones. This device required 5 layers of paper and 4 layers of tape; fluid moved from entrance to detection zone ( $\approx 5$  cm) in 5 min.

The ability to distribute samples into multiple detection zones, using 3D  $\mu\text{PADs}$  makes it possible to measure simultaneously the levels of analytes in a sample (using colorimetric assays) and to generate calibration curves for the assays. The 3D  $\mu\text{PAD}$  shown in Fig. 3 distributed each of eight  $40\text{-}\mu\text{L}$  samples into arrays of 64 detection zones. Eight different concentrations of Erioglaucine (blue dye) were added to the device, using an 8-channel pipette. Fig. 3C shows a graph of the average intensity of blue (measured as the mean intensity of cyan in CMYK format in Adobe Photoshop) in each group of 64 zones, versus the intensity of blue in the inlet spots. The small standard deviations of the measurements, and the linear relationship between the intensities at the inlet spots and the detection zones, indicated that the device evenly distributed the samples without loss due to adsorption.

The combination of camera phones and  $\mu\text{PADs}$  provides a complete system for quantitative detection of analytes in resource-limited settings (1). Three-dimensional  $\mu\text{PADs}$  generate calibration curves for comparison with unknowns by running assays on a control sample and an unknown sample side-by-side on the same device. Fig. 4 shows two prototype devices that enable this type of comparison. The first device ran assays for glucose and protein (in replicates of 4) on two different samples, and displayed the results of the sample and calibration assays in a side-by-side arrangement (Fig. 4A–D). The second device ran the same assays in duplicate, on 4 different samples: Fig. 4E–H. The reagents for the glucose and protein assays were spotted in the detection zones on the bottom layer of the device before the device was assembled. Micropipettes are not available in resource-limited environments, so the devices in Fig. 4 include sample inlets at the corners of the devices that wick fluids from corners of the device into its central region, where the samples are distributed in the vertical direction. In this format, sample volume was controlled easily by removing the device from the sample as soon as the detection zones filled (1).

## Conclusions

The combination of paper, tape, and stacking makes 3D paper-based microfluidics practical for use in resource-limited and difficult environments, and it brings new functions and capabilities to microfluidic systems. Fluids can pass vertically (both up and down) and rapidly through multiple layers of paper (each layer is only  $100\text{--}200\text{ }\mu\text{m}$  thick), and can be distributed, combined with different reagents in different layers, or filtered (as one of many possible functions).

“Paper” (loosely defined as “thin flexible sheets composed of fibrous materials”) comes in (or can be fabricated in) a wide variety of forms, with compositions ranging from cellulose to glass, polymer, or metal (16). Each type of paper can bring different functionality to a 3D  $\mu\text{PAD}$ , and thus increase its capability. The simplicity with which these devices are assembled makes the prototyping of new designs rapid, even in locations with minimal infrastructure (e.g., IDCs, where inexpensive diagnostic devices with advanced capabilities are needed most).

## Materials and Methods

**Patterning Paper.** ITW Technicloth (TX 609) was patterned with SU-8 2010 photoresist (1, 8, 9). We used ITW Technicloth wipers as the paper and ACE double-sided carpet tape, although other types of paper and tape can be used as well. Technicloth was impregnated with SU-8 2010 photoresist and pre-baked on a digital hotplate set at  $130\text{ }^{\circ}\text{C}$  for 10 min. The paper was allowed to cool to room temperature ( $23\text{ }^{\circ}\text{C}$ ) and was exposed to UV light (UVitron Intelliray 600,  $100\text{ mW}/\text{cm}^2$ ) for 14 s through a transparency mask (prepared by inkjet printing a pattern in black ink onto a transparency). Baking the paper for a second time on a digital hotplate set at  $130\text{ }^{\circ}\text{C}$  for 10 min, cooling the paper to room temperature, and washing it in a bath of acetone (1 min)



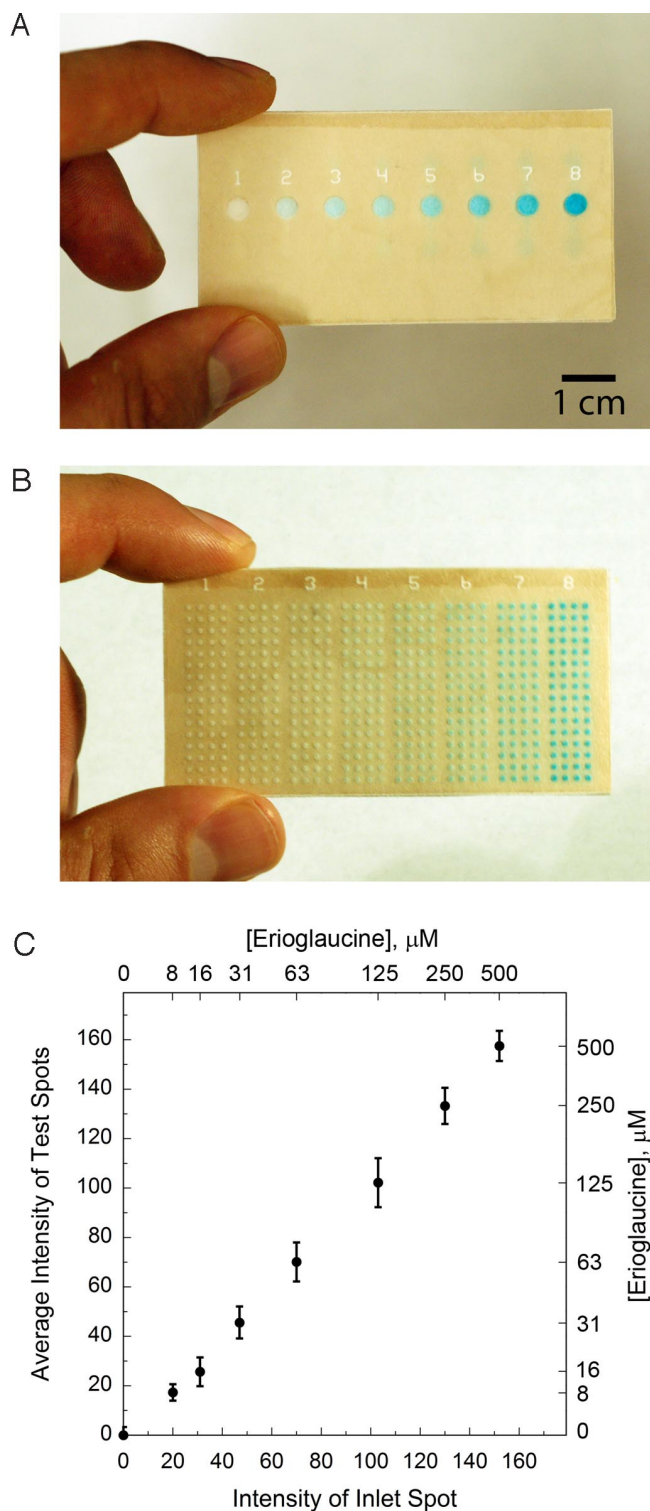


**Fig. 3.** Three-dimensional  $\mu$ PADs for running assays and generating calibration curves simultaneously, using an 8-channel micropipette. (A) Photograph of the top of the 3D  $\mu$ PAD after adding 40  $\mu$ L of 0, 8, 16, 31, 63, 125, 250, and 500  $\mu$ M Erioglaucine in water to the 8 input wells. (B) Photograph of the bottom of the 3D  $\mu$ PAD, 1 min after adding the samples to the input wells. A schematic of the layers making up the device is shown in Fig. S2. (C) Graph of average intensity of color from the test spots (measured as cyan in CMYK format in Adobe Photoshop) versus the intensity of color from the inlet spots. The results represent the average and standard deviation values from 64 replicates per sample. A related graph of average intensity of color from the test spots versus concentration of Erioglaucine is linear at low concentrations of Erioglaucine and asymptotic at high concentrations.

followed by a rinse in acetone (1 time) and a rinse in 30% water in propan-2-ol (2 times) provided patterned paper. The paper dried in 20 min under ambient conditions; after drying, it was exposed to an oxygen plasma (Harrick plasma cleaner) for 3 s at 700 millitorr to increase the hydrophilicity of the channels.

**Patterning Tape.** Double-sided tape (ACE plastic carpet tape 50106) was placed on a sheet of parchment paper. Holes were patterned into the tape, using a laser cutter (Universal Laser VL-300 50 Watt Versa Laser), using the settings for 500- $\mu$ m-thick Mylar.

**Assembling 3D  $\mu$ PADs.** We assembled the 3D devices by attaching the correctly-oriented bottom face of the double-sided tape to the bottom layer of paper. The top face of the double-sided tape remained protected by the plastic backing supplied with the tape. The holes in the tape were filled with a paste made from a mixture of cellulose powder and water [1:3 cellulose powder–water (by mass)]. The excess paste was scraped off of the plastic backing, using a metal spatula, and the plastic backing was peeled from the tape leaving the cellulose paste in the holes. The top layer of paper was attached to the top face of the tape, and the entire device was compressed by rolling 3 times with a plastic rolling pin on a bench top. The layers of tape and paper all were cut to the same dimensions before assembling the device.

**Three-Dimensional Devices for Sample Distribution.** We added 4 different aqueous dyes to the devices, using a micropipette: red (12.5 mM Allura red), blue (1 mM Erioglaucine), yellow (25 mM tartrazine), and green (0.5 mM Erioglaucine and 12.5 mM tartrazine).

**Measuring the Intensity of Colors in Adobe Photoshop.** The detection zones in the 3D devices were allowed to dry completely at 23  $^{\circ}$ C after adding the solutions of Erioglaucine with a multichannel pipette. The bottom of the device was scanned in color (EPSON Perfection 1640 SU scanner, color photo setting, 600 dpi resolution) and the image was imported into Adobe Photoshop in CMYK color mode. The intensity of color in each detection zone was measured by selecting the detection zone with the elliptical marquee tool and by recording the mean intensity of cyan, using the histogram tool. A background-corrected response was obtained by subtracting the measured intensities from the average intensity measured for detection zones that contained zero Erioglaucine (1).

**Glucose and Protein Assays.** The reagents for the glucose and protein assays were spotted and dried in their respective detection zones on the bottom layer of the device before assembling the device.

**Glucose Assay.** A reagent solution (0.2  $\mu$ L) [5:1 solution of glucose oxidase–horseradish peroxidase (120 units of glucose oxidase enzyme activity and 30 units of horseradish peroxidase enzyme activity per mL of solution), 0.6 M potassium iodide, and 0.3 M trehalose in a pH 6.0 phosphate buffer prepared in Millipore-purified water] was spotted in each glucose detection zone, using a micropipette (VWR); the paper was air-dried for 10 min at 23  $^{\circ}$ C (1). All of the reagents were purchased from Sigma–Aldrich.

**Protein Assay.** A priming solution (0.2  $\mu$ L) [92% water, 8% ethanol by volume, and 250 mM citrate buffer (pH 1.8)], was spotted on the paper, using a micropipette (VWR); this solution was allowed to air-dry for 10 min at 23  $^{\circ}$ C. A reagent solution (0.2  $\mu$ L) (95% ethanol, 5% water by volume, 9 mM tetrabromophenol blue) was spotted on top of the priming solution and dried for 10 min at room temperature (1, 17). All of the reagents were purchased from Sigma–Aldrich.

**Preparation of Standard Solutions in Artificial Urine.** We prepared an artificial urine solution as reported by Brooks and Keevil (18). The artificial urine solution contained 1.1 mM lactic acid, 2.0 mM citric acid, 25 mM sodium bicarbonate, 170 mM urea, 2.5 mM calcium chloride, 90 mM sodium chloride, 2.0 mM magnesium sulfate, 10 mM sodium sulfate, 7.0 mM potassium dihydrogen phosphate, 7.0 mM dipotassium hydrogen phosphate, and 25 mM ammonium chloride all mixed in Millipore-purified water. The pH of the solution was adjusted to 6.0 by addition of 1.0 M hydrochloric acid. All inorganic reagents were purchased from Sigma–Aldrich. Stock solutions containing the desired concentrations of glucose and BSA were prepared using this artificial urine. The stock solutions were serially diluted to the desired concentrations of glucose and BSA.

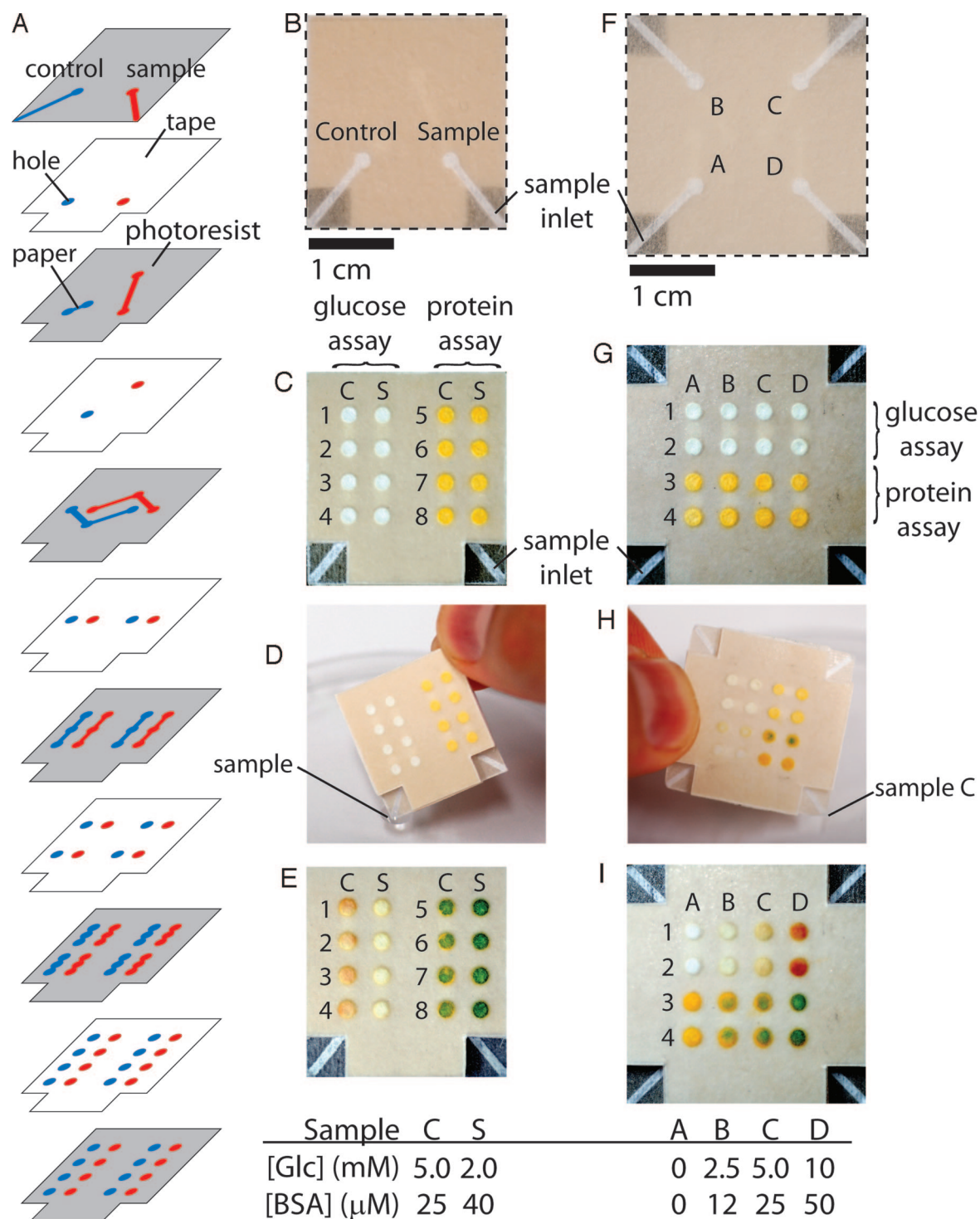


**Fig. 4.** Three-dimensional  $\mu$ PADs for running parallel assays and standards. (A) Schematic of the layers making up the device shown in B–E. (B) Photograph of the front of the dual-assay device. The sample inlets wicked the samples into the device. The dotted lines mark the edge of the device. (C) Back of the device. The reagents for colorimetric assays for glucose and proteins were prespotted in the detection zones. (D) Photograph of the device being dipped into a sample of artificial urine that contained 2-mM glucose and 40  $\mu$ M BSA. The device filled with 25  $\mu$ L of sample in 2 min. The glucose assay requires an additional 25 min to develop. (E) The results of the assays were displayed side-by-side for sample and control. The concentrations of glucose (Glc) and BSA in each sample of artificial urine are listed beneath the devices. (F) Top of a 4-assay device. (G) Back of the device. Fig. S3 shows a schematic of the layers making up the device. (H) Each corner of the device was dipped into a different sample of artificial urine. The device filled with 10  $\mu$ L of each sample within 1 min. (I) The results of the assays were displayed on the back of the device.

**Measuring the Levels of Glucose and Proteins with 3D  $\mu$ PADs.** Each sample of fluid (30  $\mu$ L) to be tested was transferred to a Petri dish, using a micropipette. The designated sample inlet on the device was dipped into the solution, and the device absorbed the solution by capillary action and distributed it into the detection zones. The device was held in the sample until all of the detection

zones were filled ( $\approx$ 2 min for the device designed for two samples, and  $\approx$ 1 min for the device designed for 4 samples). The device was removed from the sample, rotated by 90°, and the next sample inlet was dipped into its respective solution. Once all of the samples had been wicked into the device, the device was allowed to air-dry at 23 °C, and the results for the assays developed in the detection zones.

**ACKNOWLEDGMENTS.** This work was supported by the Nano/Microelectromechanical Systems Science and Technology Micro/Nano Fluidics Fundamentals Focus Center (Defense Advanced Research Projects Agency), the National Insti-

tutes of Environmental Health and Safety, The Bill and Melinda Gates Foundation, a predoctoral fellowship from the National Science Foundation (to A.W.M.), and a postdoctoral fellowship from the National Institutes of Health (to S.T.P.).

1. Martinez AW, et al. (2008) Simple telemedicine for developing regions: Camera phones and paper-based microfluidic devices for real-time, off-site diagnosis. *Anal Chem* 80:3699–3707.
2. Chin CD, Linder V, Sia SK (2007) Lab-on-a-chip devices for global health: Past studies and future opportunities. *Lab Chip* 7:41–57.
3. Daar AS, et al. (2002) Top ten biotechnologies for improving health in developing countries. *Nat Genet* 32:229–232.
4. Sia SK, et al. (2004) An integrated approach to a portable and low-cost immunoassay for resource-poor settings. *Angew Chem Int Ed Engl* 43:498–502.
5. Mabey D, et al. (2004) Diagnostics for the developing world. *Nat Rev Microbiol* 2:231–240.
6. von Lode P (2005) Point-of-care immunotesting: Approaching the analytical performance of central laboratory methods. *Clin Biochem* 38:591–606.
7. Willis RC (2006) Challenges for clinical diagnostic devices. *Anal Chem* 78:5261–5265.
8. Martinez AW, et al. (2007) Patterned paper as a platform for inexpensive, low-volume, portable bioassays. *Angew Chem Int Ed* 46:1318–1320.
9. Martinez AW, et al. (2008) FLASH: A rapid method for prototyping paper-based microfluidic devices. *Lab Chip* DOI: 10.1039/b811135a.
10. Weigl BH, et al. (2001) Design and rapid prototyping of thin-film laminate-based microfluidic devices. *Biomed Microdev* 3:267–274.
11. Bartholomeusz DA, Boutte RW, Andrade JD (2005) Xurography: Rapid prototyping of structures using a cutting plotter. *J Microelectromech Syst* 14:1364–1374.
12. Unger MA, et al. (2000) Monolithic microfabricated valves and pumps by multilayer soft lithography. *Science* 288:113–116.
13. Kartalov EP, et al. (2006) Microfluidic vias enable nested bioarrays and autoregulatory devices in Newtonian fluids. *Proc Natl Acad Sci USA* 103:12280–12284.
14. Luo Y, Zare RN (2008) Perforated membrane method for fabricating three-dimensional polydimethylsiloxane microfluidic devices. *Lab Chip* 8:1688–1694.
15. Morel CM, et al. (2005) Health innovation networks to help developing countries address neglected diseases. *Science* 309:401–404.
16. Macek K, Becvarova H (1971) Papers, ready-for-use plates, and flexible sheets for chromatography. *Chromatogr Rev* 15:1–28.
17. Pugia MJ, et al. (1999) High-sensitivity dye binding assay for albumin in urine. *J Clin Lab Anal* 13:180–187.
18. Brooks T, Keevil CW (1997) A simple artificial urine for the growth of urinary pathogens. *Lett Appl Microbiol* 24:203–206.